Effect of Bulk-Reacting Liners on Wave Propagation in Ducts

ALI HASAN NAYFEH,* JOHN SUN,† AND DEMETRI P. TELIONIS‡
Virginia Polytechnic Institute and State University, Blacksburg, Va.

An analysis is presented for the effect of bulk-reacting liners on the wave propagation and attenuation in two-dimensional and circular ducts carrying sheared mean flow. The wave propagation in an isotropic porous material lining the walls is coupled with wave propagation in the duct. The results indicate that the porosity and structure factor of the porous material have a non-negligible effect on the attenuation rate. The attenuation rate does not increase monotonically with either the liner thickness or resistivity. Considerable error may be introduced by treating a bulk-reacting liner as a point-reacting liner.

Nomenclature

c = speed of sound
c_e = effective speed of sound in porous material
d = duct half-width, see Fig. 1
F = pressure amplitude in duct, see Eq. (15)
f = pressure amplitude in liner, see Eq. (15)
h = depth of porous material
k = wave number in the z direction
k_r = real part of k
k_i = imaginary part of k
M = Mach number
p = pressure
r = radial coordinate, see Fig. 2
r_1 = radius of inner surface of duct, see Fig. 2
r_2 = radius of impermeable liner backing, see Fig. 2
t = time
u, v = z- and y-velocity components
y, z = cartesian coordinates, see Fig. 1
$\alpha = -k_i$ = attenuation rate
β = specific acoustic admittance, see Eq. (30)
γ = quantity defined in Eq. (20b)
δ = boundary-layer thickness
θ = polar coordinate, see Fig. 2
ρ = density
σ = resistivity of porous material
Ω = porosity of the lining material
ω = frequency

Subscripts and Superscripts

$*$ = dimensional quantities
$'$ = a prime denotes differentiation with respect to y
0 = mean flow quantities
1 = acoustic quantities

1. Introduction

LINING materials were long ago known and used as sound absorbers in architectural designs and industrial installations. The extreme temperature and pressure environment in the interior of a jet engine, though, has recently required extensive experimental and theoretical research to develop appropriate liners. The desirable mechanical properties of liners are diverse and rather stringent. Liners should have a minimum thickness and weight, should be able to resist high pressure levels, face extreme temperature differences, and of course, should have sufficient ability to absorb sound. These liners are usually a combination of perforated sheets, cavities, and pieces of porous materials.

In a broad classification, liners can be divided into point-reacting and bulk-reacting liners.[1] Point-reacting liners are liners that permit propagation only in the direction normal to the duct wall. They usually consist of a perforated sheet or a thin layer of porous material followed by a honeycomb core and backed by the impervious wall of the duct. The honeycomb core is made up of narrow cavities of usually polygonal shape that are directed perpendicular to the wall and the facing sheet and act as resonators. Bulk-reacting liners are liners that permit propagation in more than one direction. Such liners may consist of isotropic or anisotropic porous materials.

Whereas point-reacting liners have received considerable attention,[2,3] bulk-reacting liners have received limited attention. Analyses of the acoustical properties of bulk-reacting liners were motivated mainly by the use of fiberglass blankets as linings in air-conditioning ducts and as parallel baffles in mufflers.

Scott[4] analyzed the effect of isotropic bulk-reacting liners on the wave propagation in a two-dimensional duct without mean flow. Scott's theory was verified by several investigators.[5-9] Kurze and Vér[10] extended the analysis of Scott by considering anisotropic bulk-reacting liners. Their results show that, for low frequencies, the optimum attenuation of the lowest mode is achieved by a bulk-reacting liner whose resistivity in the axial direction increases with the frequency, in agreement with the experimental observations of Bokor.[6,7] Tack and Lambert[11] formulated the problem of wave propagation in two-dimensional ducts carrying slug flow and lined with isotropic bulk-reacting liners. No numerical results were presented. The purpose of the

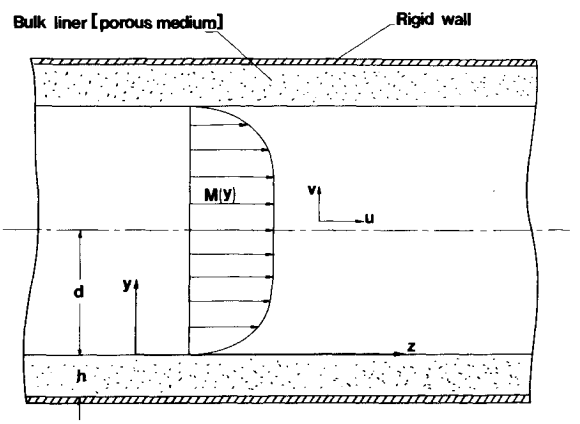

Fig. 1 A schematic of the flowfield for the two-dimensional configuration.

Presented as Paper 73-227 at AIAA 11th Aerospace Sciences Meeting, Washington, D.C., January 10–12, 1973; submitted February 1, 1973; revision received November 21, 1973. This work was supported by NASA Langley Research Center under Grant NGR 47-004-109.

Index category: Aircraft Noise, Powerplant.

* Professor of Engineering Science and Mechanics. Member AIAA.

† Research Assistant; presently, Aerospace Engineer, Naval Weapons Lab., Dahlgren, Va.

‡ Assistant Professor of Engineering Science and Mechanics. Member AIAA.

present paper is to analyze the wave propagation and attenuation in two-dimensional and circular ducts lined with isotropic bulk-reacting liners and carrying sheared mean flow.

2. Two-Dimensional Configuration

2.1 Problem Formulation

In this section, we consider the two-dimensional configuration shown in Fig. 1. We assume each flow quantity q in the duct to be the sum of a steady mean flow quantity q_0 and a fluctuating quantity q_1 where $q_1 \ll q_0$. We assume the mean flow to be fully developed and the mean density to be constant. Thus, we let

$$\begin{aligned} u^* &= u_0^*(y^*) + u_1(y^*, z^*, t^*) \\ v^* &= v_1^*(y^*, z^*, t^*) \\ p^* &= p_0^* + p_1^*(y^*, z^*, t^*) \end{aligned} \tag{1}$$

Substituting Eqs. (1) into the Euler equations and the equation of state, subtracting the mean flow terms, and neglecting nonlinear fluctuating terms, we obtain

$$\frac{\partial p_1^*}{\partial t^*} + u_0^* \frac{\partial p_1^*}{\partial z^*} + \rho_0^* c^2 \left(\frac{\partial u_1^*}{\partial z^*} + \frac{\partial v_1^*}{\partial y^*} \right) = 0 \tag{2}$$

$$\frac{\partial u_1^*}{\partial t^*} + u_0^* \frac{\partial u_1^*}{\partial z^*} + v_1^* \frac{du_0^*}{dy^*} + \frac{1}{\rho_0^*} \frac{\partial p_1^*}{\partial z^*} = 0 \tag{3}$$

$$\frac{\partial v_1^*}{\partial t^*} + u_0^* \frac{\partial v_1^*}{\partial z^*} + \frac{1}{\rho_0^*} \frac{\partial p_1^*}{\partial y^*} = 0 \tag{4}$$

where c is the speed of sound. Equations (2–4) can be combined into

$$\frac{1}{c^2} \frac{\partial^2 p_1^*}{\partial t^{*2}} = (1-M^2) \frac{\partial^2 p_1^*}{\partial z^{*2}} + \frac{\partial^2 p_1^*}{\partial y^{*2}} + 2\rho_0^* c \frac{dM}{dy^*} \frac{\partial v_1^*}{\partial z^*} - \frac{2M}{c} \frac{\partial^2 p_1^*}{\partial z^* \partial t^*} \tag{5}$$

where $M = u_0^*(y^*)/c$.

We assume the porous medium to be rigid, isotropic, and homogeneous. Also, we assume that the effect of the mean flow velocity in the porous medium is negligible provided that the resistivity of the material is not small. With these assumptions, the acoustic field in the porous medium is governed by[12]

$$\rho_e^* \frac{\partial \mathbf{u}_p^*}{\partial t^*} + \nabla^* p_p^* + \sigma^* \mathbf{u}_p^* = 0 \tag{6}$$

$$\frac{\Omega}{\rho_0^*} \frac{\partial \rho_p^*}{\partial t^*} + \nabla^* \cdot \mathbf{u}_p^* = 0 \tag{7}$$

$$p_p^* = c_e^2 \rho_p^* \tag{8}$$

where ρ_e^* is the effective density of the gas in the porous medium, Ω is the porosity, σ^* is the resistivity, and c_e is the effective speed of sound. The effective density is postulated by Zwikker and Kosten[13] to be related to the actual density by $\rho_e^* = s\rho_0^*/\Omega$, where s is called the structure factor which is mainly dependent on the structural properties of the material and the internal friction of the gas. In general, the thermal capacity of the material is much larger than that of the gas. Hence, at low frequencies, the compression and rarefaction of the gas as the acoustic wave propagates through the material are slow enough so that the conduction process maintains the gas at a constant temperature; consequently, $c_e^2 = \partial p/\partial \rho$ at constant temperature. However, at high frequencies, the compression and rarefaction take place so rapidly that the conduction process is insignificant and the compression and rarefaction process is essentially adiabatic; consequently, $c_e^2 = \partial p/\partial \rho$ at constant entropy.[12] At the intermediate frequencies, the compression and rarefaction process is neither isothermal nor adiabatic; consequently $c_e^2 = \partial p/\partial \rho$ with neither the temperature nor the entropy kept constant. In the latter case, c_e is a complex number as compared with the low and high frequency cases when it is real. The resistivity of the material is a function of the gas viscosity, pore size, porosity, structure factor, and the acoustic frequency if it is high.[14,15] Thus, ρ_e^*, Ω, and σ^* are not independent but related. However, their interdependence is complicated so that they, in general, are determined separately.[3]

Equations (6–8) can be combined into

$$\frac{s}{c_e^2} \frac{\partial^2 p_p^*}{\partial t^{*2}} + \frac{\sigma^* \Omega}{\rho_0^* c_e^2} \frac{\partial p_p^*}{\partial t^*} - \nabla^{*2} p_p^* = 0 \tag{9}$$

To complete the problem formulation, we need to specify the boundary conditions. At the rigid walls, the normal component of velocity vanishes; that is

$$v_p^*(-h^*, z^*, t^*) = 0 \tag{10}$$

At the interface separating the flows in the duct and the porous medium, the pressure and particle displacement are continuous. The first condition yields

$$p_1^*(0, z^*, t^*) = p_p^*(0, z^*, t^*) \tag{11}$$

If the interface is given by $y^* = \eta(z^*, t^*)$, the linearized form of the continuity of the particle displacement leads to

$$\begin{aligned} &\eta_t + u_0^* \eta_z = v_1^* \\ &\eta_t = v_p^* \end{aligned} \quad \text{at} \quad y^* = 0 \tag{12}$$

If u_0^* vanishes at the wall, Eq. (12) reduces to the continuity of the normal velocity at the interface. If the properties of the porous material are the same on both sides of the duct, the boundary condition at the upper wall can be replaced by a boundary condition at the center of the duct; that is

$$\begin{aligned} p_1^*(d^*, z^*, t^*) &= 0 \quad \text{for antisymmetric modes} \\ \partial p_1^*(d^*, z^*, t^*)/\partial y^* &= 0 \quad \text{for symmetric modes} \end{aligned} \tag{13}$$

2.2 Modal Analysis

Before carrying out the modal analysis, we introduce dimensionless variables using the characteristic length d^*, the characteristic speed c, and the ambient density ρ_0^*. Thus, we let

$$\begin{aligned} t &= t^* c/d^*, \quad z = z^*/d^*, \quad y = y^*/d^* \\ h &= h^*/d^*, \quad \omega = \omega^* d^*/c \\ u &= u^*/c, \quad v = v^*/c, \quad p = p^*/\rho_0^* c^2 \end{aligned} \tag{14}$$

Then, we assume the following modal solution

$$\begin{aligned} p_1(y, z, t) &= F(y)E, \quad v_1(y, z, t) = G(y)E \\ p_p(y, z, t) &= f(y)E, \quad v_p(y, z, t) = g(y)E \end{aligned} \tag{15}$$

where

$$E = \exp[i(\omega t - kz)] \tag{16}$$

Here, k is a complex constant whose real part k_r represents the dimensionless wave number and its imaginary part k_i represents the negative of the dimensionless attenuation rate. Substituting Eqs. (14–16) into Eqs. (4–6) and (9–12), we obtain

$$F' + i(\omega - Mk)G = 0 \tag{17}$$

$$F'' - 2iM'kG + [(\omega - Mk)^2 - k^2]F = 0 \tag{18}$$

$$\left(\sigma + \frac{i\omega s}{\Omega} \right) g + f' = 0 \tag{19}$$

$$f'' + \gamma^2 f = 0 \tag{20a}$$

$$\gamma^2 = -k^2 + \frac{sc^2\omega^2}{c_e^2} - i\frac{\sigma\omega\Omega c^2}{c_e^2} \tag{20b}$$

$$g(-h) = 0 \tag{21}$$

$$F(0) = f(0) \tag{22}$$

$$G(0) = g(0) \tag{23}$$

where $\sigma = \sigma^* d^*/\rho_0^* c$ and primes denote differentiation with respect to y. In arriving at Eq. (23), we used the noslip condition of the mean flow; that is, $M(0) = 0$.

Eliminating G from Eqs. (17) and (18), we obtain

$$\frac{d^2F}{dy^2} + \frac{2M'k}{\omega - Mk} \frac{dF}{dy} + [(\omega - Mk)^2 - k^2]F = 0 \tag{24}$$

Using Eqs. (17) and (19), we rewrite the boundary conditions (21) and (23) as

$$f'(-h) = 0 \tag{25}$$

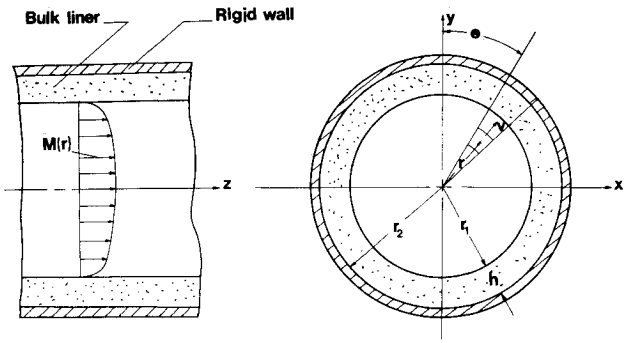

Fig. 2 A schematic of the flowfield for the cylindrical configuration.

$$F'(0) = i\omega\left(\sigma + \frac{is\omega}{\Omega}\right)^{-1} f'(0) \tag{26}$$

The solution of Eq. (20) subject to the boundary condition (25) is

$$f = a\cos\gamma(y+h) \tag{27}$$

where a is an arbitrary constant. Equation (20b) shows that γ is complex, and therefore the expression (27) has a factor of the form $\exp(ik_y y)$ which corresponds to plane wave propagation normal to the wall in the lining. Substituting for f into Eqs. (22) and (26), we obtain

$$F(0) = a\cos\gamma h$$

$$F'(0) = -ia\omega\gamma\left[\sigma + \frac{is\omega}{\Omega}\right]^{-1}\sin\gamma h$$

Eliminating a from these equations, we have

$$F'(0) = -i\omega\gamma\left[\sigma + \frac{is\omega}{\Omega}\right]^{-1}\tan\gamma h F(0) \tag{28}$$

The symmetry boundary conditions (13) become

$$\begin{aligned} F(1) &= 0 \quad \text{for antisymmetric modes} \\ F'(1) &= 0 \quad \text{for symmetric modes} \end{aligned} \tag{29}$$

Thus, the problem is reduced to the solution of the eigenvalue problem consisting of the differential Eq. (24) subject to the boundary conditions (28) and (29) for the complex eigenvalue k and the eigenfunction F. Note that the effect of the bulk liner has been reduced to the boundary condition (28). Therefore, the bulk liner specific admittance is

$$\beta = -\omega\gamma\left[\sigma + \frac{is\omega}{\Omega}\right]^{-1}\tan\gamma h \tag{30}$$

Moreover, the eigenvalue k appears in the boundary condition (through γ) as well as in the differential equation. Thus, the acoustic field in the duct is coupled with the acoustic field in the liner.

For a one-dimensional lining material that allows propagation normal to the wall only, the wall admittance can be obtained by letting $k = 0$ in Eqs. (20b) and (30); that is

$$\tilde{\beta} = -\omega\tilde{\gamma}\left[\sigma + \frac{is\omega}{\Omega}\right]^{-1}\tan\tilde{\gamma}h \tag{31}$$

where

$$\tilde{\gamma}^2 = (sc^2\omega^2/c_e^2) - i(\sigma\omega\Omega c^2/c_e^2)$$

Note that this liner is a point-reacting liner without an air cavity.

3. Cylindrical Configuration

In this case, Eqs. (4) and (5) become

$$\frac{\partial v_1^*}{\partial t^*} + u_0^*\frac{\partial v_1^*}{\partial z^*} + \frac{1}{\rho}\frac{\partial p_1^*}{\partial r^*} = 0 \tag{32}$$

$$\frac{1}{c^2}\frac{\partial^2 p_1^*}{\partial t^{*2}} = \nabla^2 p_1^* - M^2\frac{\partial^2 p_1^*}{\partial z^{*2}} + 2\rho_0^* c\frac{dM}{dr^*}\frac{\partial v_1^*}{\partial z^*} - \frac{2M}{c}\frac{\partial^2 p_1^*}{\partial z^*\partial t^*} \tag{33}$$

We introduce dimensionless quantities as in the previous case except that d is replaced by r_1, and assume a solution of the form

$$\begin{aligned} p_1^* &= \rho_0^* c^2 F(r)E, \quad v_1^* = cG(r)E \\ p_p^* &= \rho_0^* c^2 f(r)E, \quad v_p^* = cg(r)E \end{aligned} \tag{34}$$

where

$$E = \exp[i(\omega t - kz + m\theta)] \tag{35}$$

and r, θ, and z are the dimensionless cylindrical coordinates shown in Fig. 2.

Substituting Eqs. (34) and (35) into Eqs. (6, 9, 32, and 33), we have

$$\left[\sigma + \frac{i\omega s}{\Omega}\right]g + f' = 0 \tag{36}$$

$$\frac{d^2 f}{dr^2} + \frac{1}{r}\frac{df}{dr} + \left[\gamma^2 - \frac{m^2}{r^2}\right]f = 0 \tag{37}$$

$$i(\omega - Mk)G + F' = 0 \tag{38}$$

$$\frac{d^2 F}{dr^2} + \left[\frac{1}{r} + \frac{M'k}{\omega - Mk}\right]\frac{dF}{dr} + \left[(\omega - Mk)^2 - k^2 - \frac{m^2}{r^2}\right]F = 0 \tag{39}$$

where primes denote differentiation with respect to r and γ is defined in Eq. (20b). The boundary conditions (21–23) becomes

$$\begin{aligned} g(r_2) &= 0 \\ F(1) &= f(1) \\ G(1) &= g(1) \end{aligned} \tag{40}$$

Using Eqs. (36) and (38), we rewrite the boundary conditions (40) as

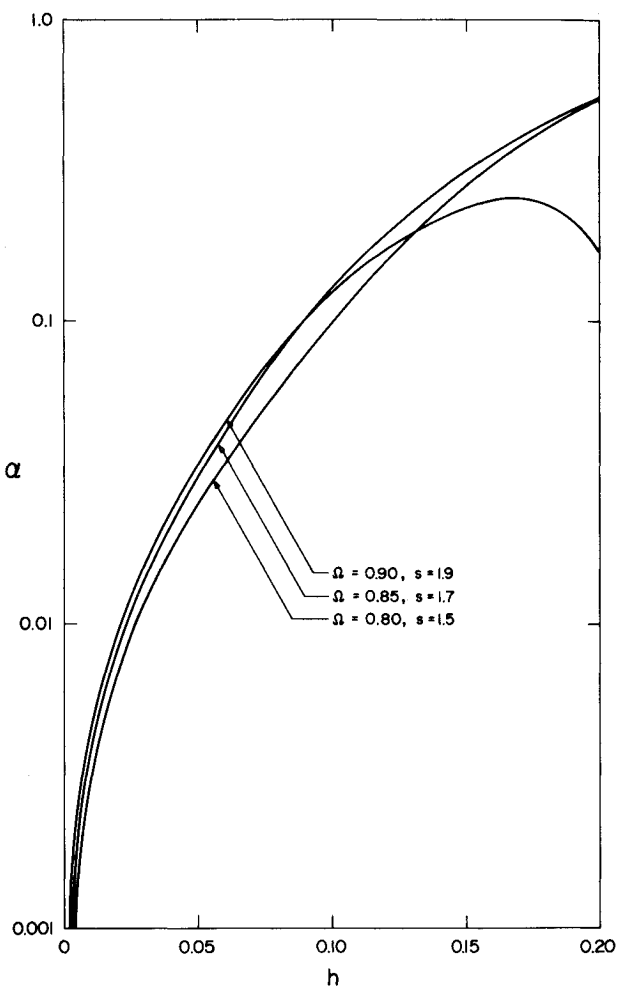

Fig. 3 Variation of the attenuation rate with the liner thickness for the two-dimensional configuration, $\sigma = 12.92$ and $\omega = 4$.

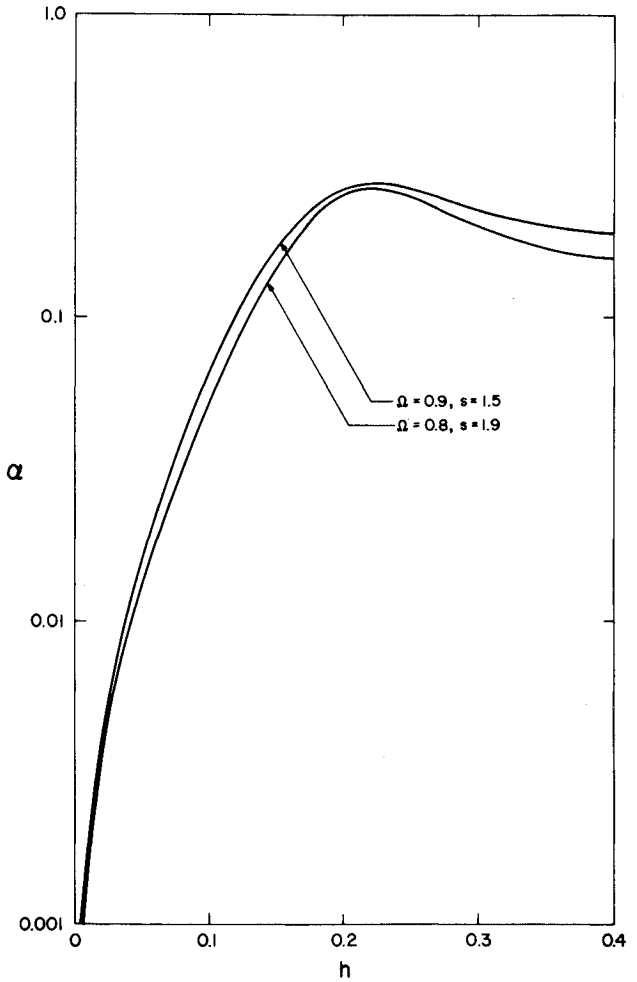

Fig. 4 Variation of the attenuation rate with the liner thickness for the cylindrical configuration, $\sigma = 12.92$ and $\omega = 4$.

$$\begin{aligned} f'(r_2) &= 0 \\ F(1) &= f(1) \\ F'(1) &= i\omega\left[\sigma + \frac{i\omega s}{\Omega}\right]^{-1} f'(1) \end{aligned} \tag{41}$$

The solution of Eq. (37) subject to the first boundary condition in (41) is

$$f = a[J_m(\gamma r) + bY_m(\gamma r)] \tag{42}$$

where J_m and Y_m are the mth-order Bessel functions of the first and second kind, respectively, and

$$b = -J_m'(\gamma r_2)/Y_m'(\gamma r_2) \tag{43}$$

Substituting for f into the last two boundary conditions in Eq. (41) and eliminating a, we obtain

$$\frac{F'(1)}{F(1)} = i\omega\gamma\left[\sigma + \frac{i\omega s}{\Omega}\right]^{-1} \frac{J_m'(\gamma)Y_m'(\gamma r_2) - J_m'(\gamma r_2)Y_m'(\gamma)}{J_m'(\gamma)Y_m'(\gamma r_2) - J_m'(\gamma r_2)Y_m(\gamma)} \tag{44}$$

Thus, the problem is reduced to the solution of the eigenvalue problem consisting of the differential equation (39) subject to the boundary condition (44) and $F(0) < \infty$. As in the two-dimensional case, the analysis of a one-dimensional point-reacting liner without an air cavity is the same as for the bulk liner except $k = 0$ in Eq. (20b).

4. Numerical Analysis

In the numerical calculations we used

$\rho_0{}^* = 0.0773$ lb/ft^3, $c = c_e = 1000$ fps, $M_0 = 0.3$, $\delta = 0.1$

where δ is the dimensionless boundary-layer thickness of the mean flow.

4.1 Two-Dimensional Case

The eigenvalue problem consisting of Eqs. (24, 28, and 29) was solved numerically. The following mean flow velocity profile proposed by Savkar[16] was used

$$\begin{aligned} M &= M_0 y/(1-0.5\delta) \quad \text{for} \quad 0 \leqq y \leqq \delta \\ M &= M_0/(1-0.5\delta) \quad \text{for} \quad \delta \leqq y \leqq 1 \end{aligned} \tag{45}$$

For a given σ, s, Ω, and h we guessed a value for k. Letting $F(0) = 1$ in Eq. (28) we integrated Eq. (24) from $y = 0$ to $y = 1$ using a fourth-order Runge-Kutta scheme. The resulting solution at $y = 1$ was checked to see whether it satisfied the symmetry condition (29). If this condition was not satisfied, a new guess was used for k using a Newton-Raphson technique, and the procedure was repeated until the symmetry condition was satisfied to within a prescribed accuracy.

4.2 Cylindrical Case

In performing the calculations for this case, we used the following velocity profile:

$$\begin{aligned} M &= M_0 \sin[\pi(r-1+2\delta)/2\delta] \quad \text{for} \quad 1-\delta \leqq r \leqq 1 \\ M &= M_0 \quad \text{for} \quad r \leqq 1-\delta \end{aligned} \tag{46}$$

Rather than marching from the wall to the center of the duct, we marched outward from the center to avoid the solution which is singular at the origin. Moreover, we used the analytical approximation $F = r^m$ for $r \ll 1$ to calculate the initial conditions at $r = 0.01$. We guessed a value for k and integrated Eq. (39) using a fourth-order Runge-Kutta scheme outward to $r = 1$. Then, we checked to see whether the resulting solution satisfied the boundary condition (44). If this condition was not satisfied, we guessed a new value for k using a Newton-Raphson technique and repeated the procedure until the boundary condition was satisfied to within a prescribed accuracy.

4.3 Results

Figures 3 and 4 show the variation of the dimensionless attenuation rate $\alpha = -k_i$ for the lowest acoustic mode with the liner thickness h for the two-dimensional and cylindrical configurations, respectively. These figures indicate that as the thickness increases starting from zero, the attenuation rate increases from zero, attains a maximum and then slowly decreases. Note

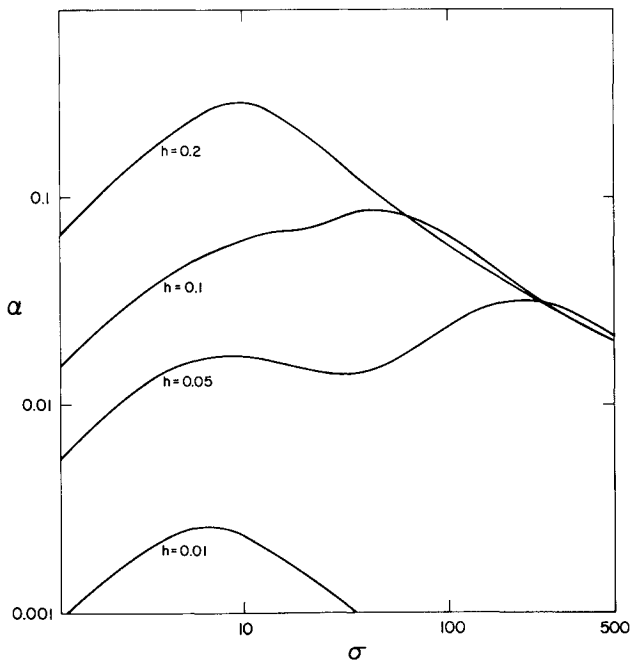

Fig. 5 Variation of the attenuation rate with the resistivity for the two-dimensional configuration, $\Omega = 0.9$, $s = 1.5$, and $\omega = 4$.

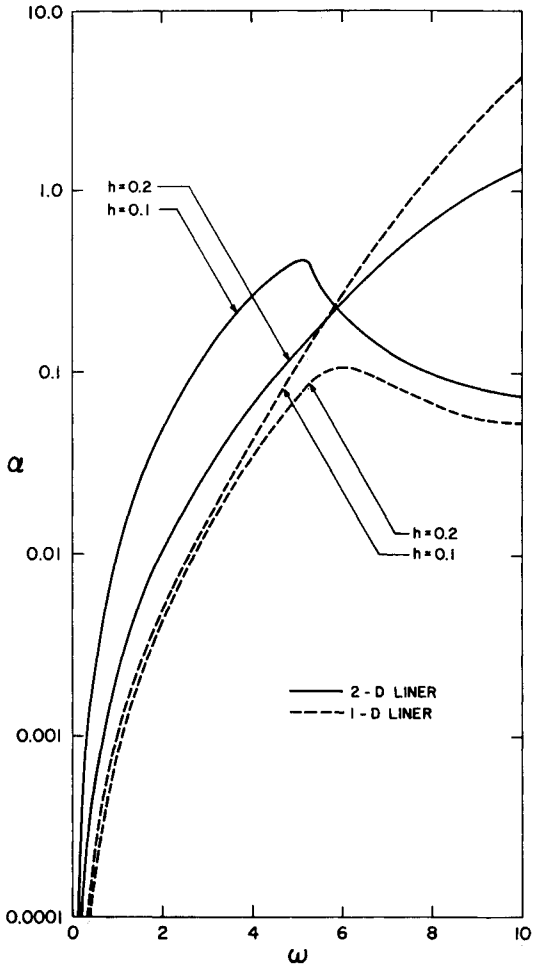

Fig. 6 Comparison of the attenuation rate of the lowest mode for two- and one-dimensional liners ($\Omega = 0.9$, $s = 1.5$, $\sigma = 12.92$, and the two-dimensional configuration).

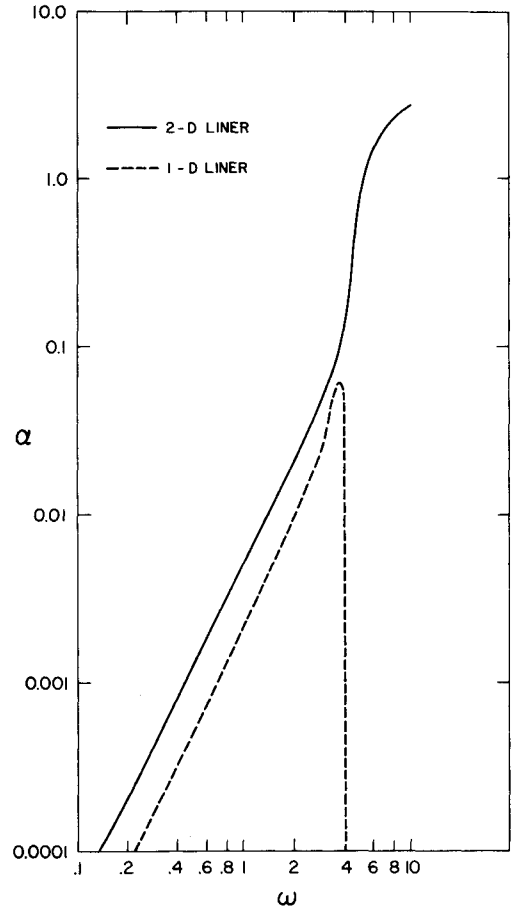

Fig. 7 Comparison of the attenuation of the lowest mode for two- and one-dimensional liners ($\Omega = 0.9$, $h = 0.1$, $s = 1.5$, $\sigma = 12.92$ and the cylindrical configuration).

also that the porosity and the structure factor have a non-negligible effect on the attenuation rate.

Figure 5 shows the variation of the attenuation rate for the lowest mode with the dimensionless resistivity σ. Again it was found that as σ increases from zero, the attenuation rate increases from zero to one or more maxima and then decreases slowly to zero. This behavior may be explained by the fact that the extreme values, $\sigma = 0$ and $\sigma \to \infty$, of the resistivity correspond to rigid walls at $y = -h$ and $y = 0$, respectively.

Figures 6–8 show that considerable error may be introduced by treating a bulk-reacting liner (two-dimensional liner) as a point-reacting liner without a cavity (one-dimensional liner). Figures 6 and 7 show that bulk-reacting liners attenuate the lowest mode more than one-dimensional liners at low frequencies in both the two-dimensional and cylindrical configurations. This is in qualitative agreement with the experimental observations of Scott[4] and the theoretical results of Kurze and Vér[11] for no mean flow. Figure 8 shows that, at least for the range of parameters studied, bulk reacting liners attenuate the second mode more than one-dimensional liners for all frequencies.

Figure 9 compares the performance of one- and two-dimensional liners as a function of the liner thickness and material resistivity. It appears that two-dimensional liners are better sound absorbers than one-dimensional liners for small thicknesses and equal material properties. However, the reverse is true for large liner thicknesses and small material resistivity. The variation of attenuation rate with resistivity, though, is not monotonic as shown in Figs. 3 and 4.

The present results do not compare the optimal performances of bulk-reacting and point-reacting liners. To compare their

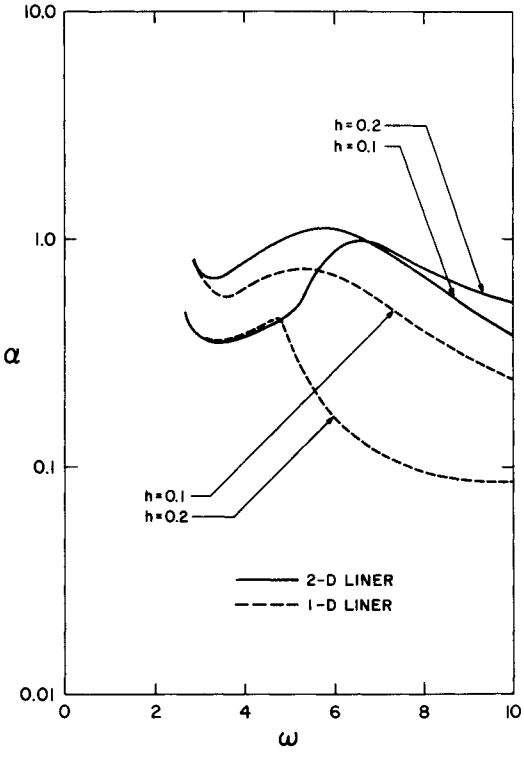

Fig. 8 Comparison of the attenuation of the second mode for two- and one-dimensional liners ($\Omega = 0.9$, $s = 1.5$, $\sigma = 12.92$, and the two-dimensional configuration).

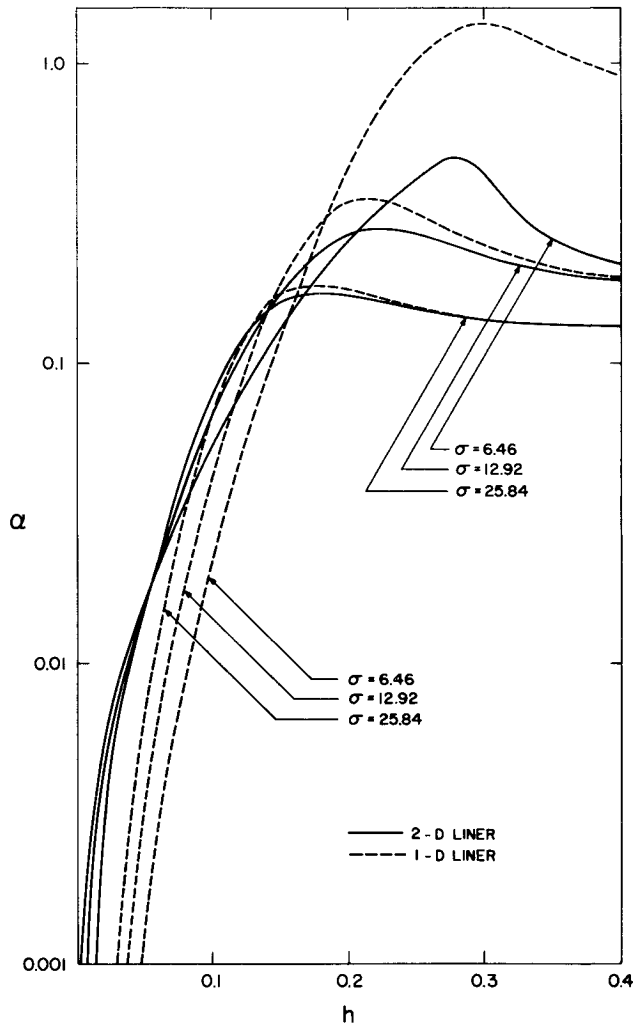

Fig. 9 Comparison of the attenuation of the lowest mode for two- and one-dimensional liners ($\Omega = 0.9, s = 1.5, \omega = 4$, and the two-dimensional configuration).

performances at given frequencies, one should vary the parameters of each liner until the maximum attenuation rate is obtained and then compare the resulting maxima.

5. Summary

The wave propagation in a bulk-reacting liner is coupled with the wave propagation in a two-dimensional or circular duct carrying sheared mean flow. The problem is reduced to the solution of the wave propagation in the duct subject to a wall admittance which depends on the liner thickness, resistivity and porosity as well as the propagation constant. The solution of this problem is obtained numerically using a combination of a Newton-Raphson technique and a fourth-order Runge-Kutta integration scheme.

The results show that the attenuation rate does not increase monotonically with either the liner thickness or resistivity. Thus, at each frequency, an optimum thickness and resistivity can be calculated. The material porosity and structure factor have a non-negligible effect on the attenuation rate.

The results show that considerable error may be introduced by treating a two-dimensional liner as a one-dimensional liner, especially for the higher modes and the lowest mode at low frequencies. It appears that an optimum liner can be obtained using a combination of a bulk-reacting liner and a point-reacting liner. An extensive parametric study needs to be performed to determine the optimum liner configuration.

References

[1] Mangiarotty, R. A., "Acoustic-Lining Concepts and Materials for Engine Ducts," *The Journal of the Acoustical Society of America*, Vol. 48, No. 3, Sept. 1970, pp. 783–794.

[2] Hubbard, H. H., Lansing, D. L., and Runyan, H. L., "A Review of Rotating Blade Noise Technology," *Journal of Sound and Vibration*, Vol. 19, No. 3, Dec. 1971, pp. 227–249.

[3] Nayfeh, A. H., Kaiser, J. E., and Telionis, D. P., "The Acoustics of Aircraft Engine-Duct Systems," AIAA Paper 73-1153, Montreal, Canada, 1973.

[4] Scott, R. A., "The Absorption of Sound in a Homogeneous Porous Medium," *Proceedings of the Physical Society* (London), Vol. 58, 1946, pp. 165–183.

[5] Leskov, E. A., Osirov, G. L., and Yudin, E. J., "Experimental Investigations of Splitter Duct Silencers," *Applied Acoustics*, Vol. 3, No. 1, Jan. 1970, pp. 47–56.

[6] Bokor, A., "Attenuation of Sound in Lined Ducts," *Journal of Sound and Vibration*, Vol. 10, No. 3, Nov. 1969, pp. 390–403.

[7] Bokor, A., "A Comparison of Some Acoustic Duct Lining Material, According to Scott's Theory," *Journal of Sound and Vibration*, Vol. 14, No. 3, Feb. 1971, pp. 367–373.

[8] Walsdorff, J., "Absorptionsschalldämpfer ohne Kassettierung," Paper 25A6, 1971, Seventh International Congress on Acoustics, Budapest, Hungary.

[9] Mongy, M., "Acoustical Properties of Porous Materials," *Acustica*, Vol. 28, No. 4, April 1973, pp. 243–247.

[10] Kurze, U. J. and Vér, I. L., "Sound Attenuation in Ducts Lined with Non-Isotropic Material," *Journal of Sound and Vibration*, Vol. 24, No. 2, Sept. 1972, pp. 177–187.

[11] Tack, D. H. and Lambert, R. F., "Influence of Shear Flow on Sound Attenuation in a Lined Duct," *The Journal of the Acoustical Society of America*, Vol. 38, No. 4, Oct. 1965, pp. 655–666.

[12] Morse, P. M. and Ingard, K. U., *Theoretical Acoustics*, McGraw-Hill, New York, 1968, pp. 252–255.

[13] Zwikker, C. and Kosten, C. W., *Sound Absorbing Materials*, Elsevier, New York, 1949.

[14] Green, L. and Duwez, P., "Fluid Flow Through Porous Metals," *Transactions of ASME, Journal of Applied Mechanics*, Vol. 18, No. 1, March 1951, pp. 39–45.

[15] Bies, D. A., "Acoustical Properties of Porous Materials," in *Noise and Vibration Control*, edited by L. L. Beranek, McGraw-Hill, New York, 1971, pp. 245–269.

[16] Savkar, S. D., "Propagation of Sound in Ducts with Shear Flow," *Journal of Sound and Vibration*, Vol. 19, No. 3, Dec. 1971, pp. 355–372.